

# Contents

<b>Introduction</b>	<b>2</b>
<b>Investigation 1</b>	
<b>(Effect of parameters on the ice-age state)</b>	<b>2</b>
(a) Hysteresis in Solar Constant . . . . .	2
(b) Investigating changes in $k$ . . . . .	2
(c) Investigating changes in $T_c$ . . . . .	3
(d) Varying Parameters A and B . . . . .	4
<b>Investigation 2</b>	
<b>(Search for other steady-state solutions)</b>	<b>5</b>
(a) Asymmetric Steady States . . . . .	5
(b) Continuous Albedo Function . . . . .	6
<b>Investigation 3</b>	
<b>(Incorporating real diffusion)</b>	<b>7</b>
(a) Formulating real diffusion . . . . .	7
(b) Investigating model changes . . . . .	7
Varying The Solar Constant . . . . .	8
Varying The Thermal Diffusivity . . . . .	9
<b>Conclusion</b>	<b>9</b>

# Introduction

**The gulf stream will shut down, Causing the Earth to freeze...**<sup>[1]</sup> Good news for Scrat!<sup>[2]</sup> Not really though, according to Oceanographers at Woods Hole Oceanographic Institution<sup>[3]</sup>. The misnomer comes from an over simplification of a model for the currents that drive global climate. This does however serve a good lesson in the importance of analysis regarding complex climate models.

In this report we aim to investigate the use of an Energy Balance Model (EBM) in the context of modelling temperature distribution and climate change on Earth. We hope to provide insight into the model's dynamics, sensitivity to changes, limitations, and analyse model improvements. We consider the possibility of asymmetric steady states about the equator, their effects on the model and introduce a continuous albedo function. We also consider the use of a real diffusion model for energy transport studying how this affects our EBM. We cite multiple sources throughout our discussions to aid the reader in their understanding as well as provide much-needed context to our calculations.

## Investigation 1

### (a) Hysteresis in Solar Constant

We begin by investigating the effect of the solar constant on the current state of Earth, as shown in the below figure:

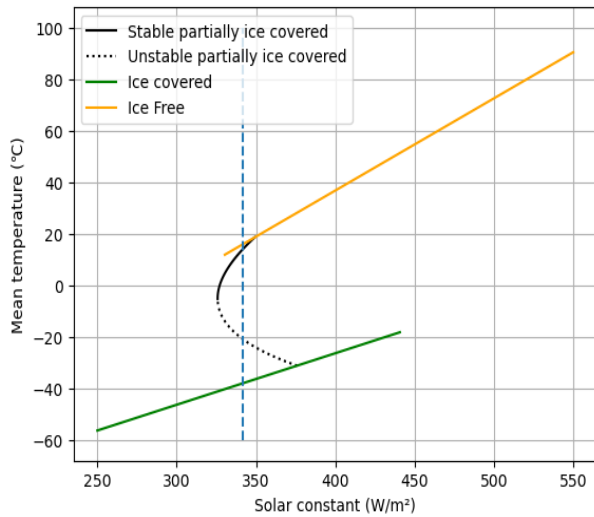


Figure 1: Evolution of state of the Earth

We start at the Earth's current partially-iced state with ice line  $y_s \approx 0.939$  and solar constant  $Q = 342W/m^2$ . In order for the Earth to fully glaciare, the solar constant needs to decrease to  $Q \approx 325.8W/m^2$ , requiring a drop of

$16.2W/m^2$ . Past this tipping point, the system exhibits hysteresis and shifts from a previous ice line of  $y_s \approx 0.6$  to a fully glaciared state.

Now, the solar constant must increase by  $115.2W/m^2$  to  $Q \approx 441W/m^2$  in order for the full-ice steady state to vanish. The system again exhibits hysteresis and ice retreats from the equator with the system now in an ice-free state.

### (b) Investigating changes in $k$

The aim of this section is to analyse how the climate is affected by varying the transport parameter,  $k$ . We start by using asymptotic analysis to estimate solutions for both  $k \ll 1$  and  $k \gg 1$ . Using the mean temperature equation from lectures as stated later 1 and given  $k \ll 1$ , we expand the solution as:

$$T_\infty(y) = T_0(y) + kT_1(y) + k^2T_2(y) + \dots$$

and, after grouping orders of  $k$ , we take a leading term approximation:

$$T_\infty(y) \sim T_0(y) = \frac{Q}{B}[s(y)(1 - a(y))] - \frac{A}{B}.$$

Similarly for  $k \gg 1$ , but instead taking the expansion:

$$T_\infty(y) = T_0(y) + \epsilon T_1(y) + \epsilon^2 T_2(y) + \dots$$

where  $\epsilon = \frac{1}{k} \ll 1$ . Again, taking the leading term after grouping gives:

$$T_\infty(y) \sim T_0(y) = \frac{Q}{B}(1 - \bar{a}) - \frac{A}{B}.$$

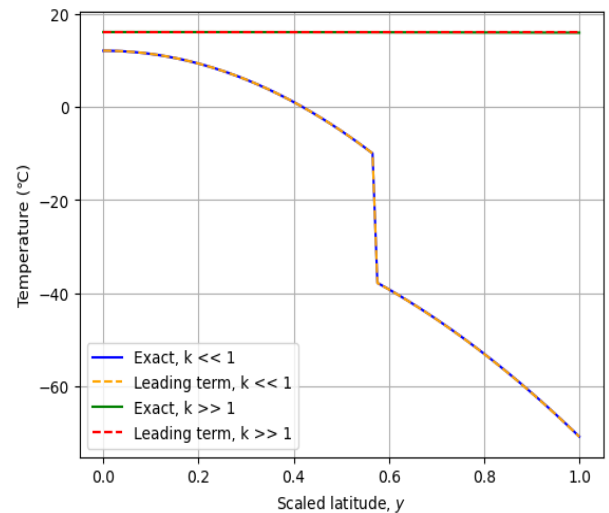


Figure 2: Temperature steady states for varied transport parameter

The above graph 2 shows that the leading term

approximations are very accurate to the exact solution. For a  $k \ll 1$ , the temperature has much greater variation across latitudes as expected with negligible heat transfer across the globe. Furthermore, the ice line was calculated to be at  $y_s \approx 0.566$ , much closer to the equator as heat is unable to spread north into the colder regions. In contrast, for  $k \gg 1$  the temperature across all latitudes is constant as the heat transport dominates the model.

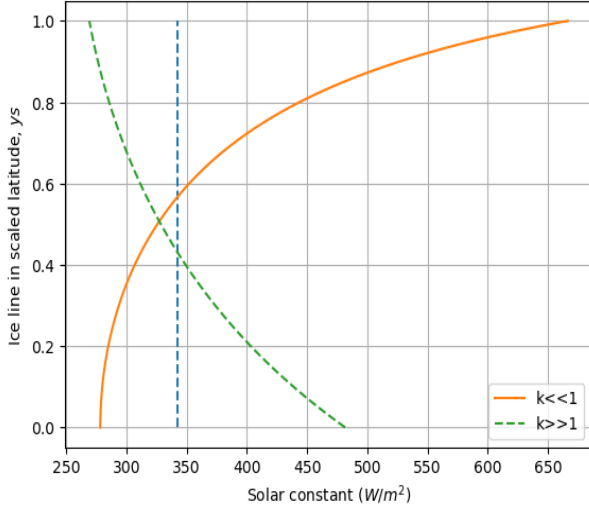


Figure 3: Ice line steady states for varied transport parameter and solar constant

We further investigate by looking at the impact of changing the solar constant on both of these climates as shown in the above figure 3. With  $k \ll 1$ , a much larger change in the solar constant is required for the ice line to retreat or expand. Whereas with  $k \gg 1$ , figure 3 shows the unstable ice line within these latitudes, with the current stable state being ice-free. Only a significant reduction in  $Q$  would result in ice forming and we would expect the ice line to rapidly expand into a fully glaciated state if  $Q$  continued to decrease.

### (c) Investigating changes in $T_c$

We continue by investigating the effect of the critical temperature,  $T_c$ , on the climate. The critical temperature is the temperature at which ice forms and we assume the ice line begins at this temperature. Therefore, by varying our model from the original value of  $T_c = -10^\circ\text{C}$  we can analyse the impact on Earth, as demonstrated in Figure 4.

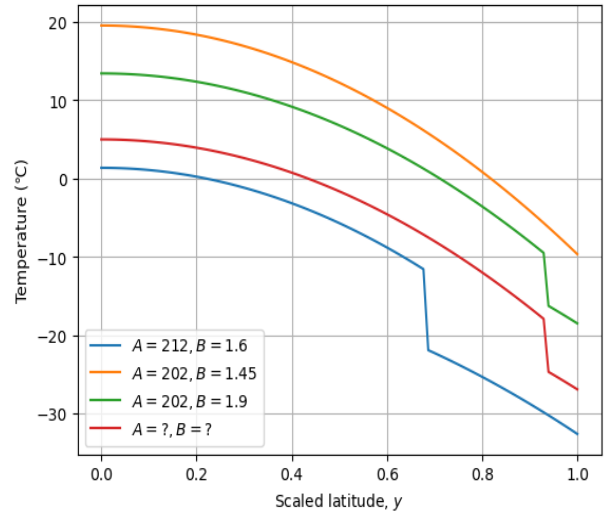


Figure 4: Temperature steady states for varied critical temperature

As expected, an increase in critical temperature would result in an increase of ice coverage, with the ice line expanding from the North Pole down to the equator. Additionally, this leads to a greater difference between the mean temperatures of the ice-covered latitudes and the exposed sea/land. When increasing the critical temperature past  $T_c = -6^\circ\text{C}$  the solution for the ice line no longer converges which could be as a result of the critical temperature being unable to coincide with the solar constant of  $Q = 342\text{W}/\text{m}^2$  as shown in Figures 5 and 6.

On the other hand, decreasing the critical temperature reduces the ice covered latitudes and the change in albedo increases the temperature of these areas. A critical temperature of less than  $T_c = -12^\circ\text{C}$  would result in an ice-less state of the Earth.

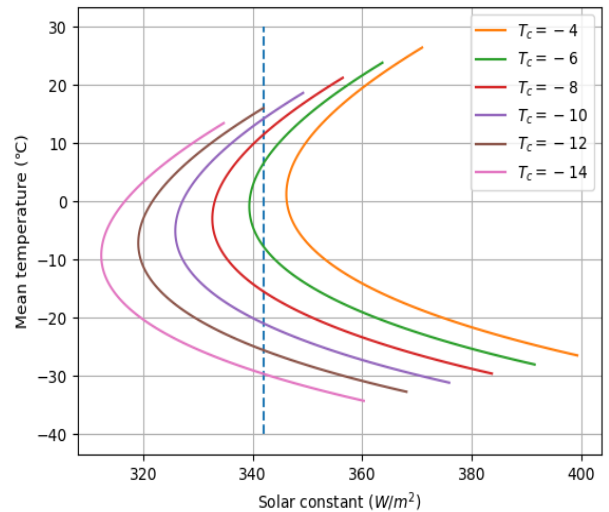


Figure 5: Temperature steady states for varied critical temperature and solar constant

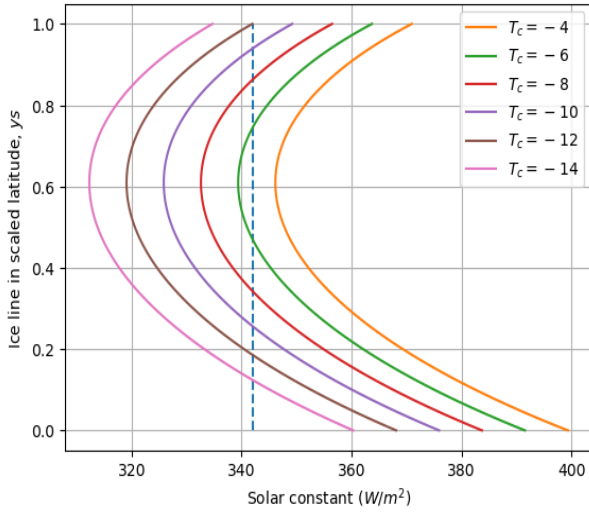


Figure 6: Ice line steady states for varied critical temperature and solar constant

We further looked at the impact of the critical temperature on the climatic sensitivity to changing the solar constant. Figure 5 and 6 suggest that the critical temperature does not affect the climatic sensitivity to changing the solar constant with the rate of change similar in respect to the ice line and global mean temperature.

#### (d) Varying Parameters A and B

In this section, we consider the effect on the climate by varying the parameters  $A$  and  $B$  which govern the total output energy of the planet,  $E_{\text{out}}(y, t) = A + BT$ . One would expect to see, for a fixed value of the solar constant  $Q_0 = 342 \text{ W m}^{-2}$ , the position of the ice line to change given different values of  $A$  and  $B$ , detailed in the plot below:

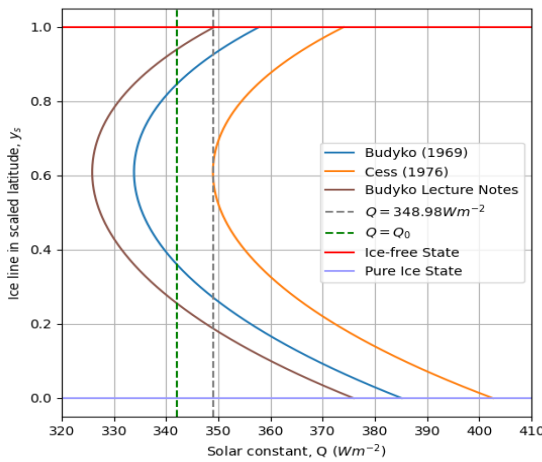


Figure 7: Ice line steady states for varied solar constant and differing parameter values of  $A$  and  $B$

As one can see from Figure 7, given Budyko's original parameter values of  $A = 202 \text{ W m}^{-2}$  and  $B = 1.45 \text{ W m}^{-2} \text{ } ^\circ\text{C}^{-1}$ , the stable value for the mixed-state ice line is decreased to  $y_s \approx 0.846$  compared to the value of  $y_s \approx 0.939$  from Budyko's later values provided in the lecture notes. This means, given an ice line positioned further south as predicted by such  $A$  and  $B$ , we would expect to see a colder overall projected climate as compared to the climate model we get from Budyko's later proposed constants. However, given the same fixed value for the solar constant of  $Q_0 = 342 \text{ W m}^{-2}$ , the model formed by Cess' 1976 parameters,  $A = 212 \text{ W m}^{-2}$  and  $B = 1.6 \text{ W m}^{-2} \text{ } ^\circ\text{C}^{-1}$ , no longer has a possible mixed-state value for the ice line. From Figure 7, we can see it would require a minimum value for the solar constant of  $Q \approx 349 \text{ W m}^{-2}$  to form a mixed-state solution for the ice line, positioned at  $y_s \approx 0.609$ . This means these parameter values predict an ice-covered state given the same value for the solar constant, resulting in the ice line being positioned at the equator ( $y_s = 0$ ). We can now model the steady state temperature against the latitude coordinate  $y$  for these different cases that arise from the choices of the parameter values  $A$  and  $B$ :

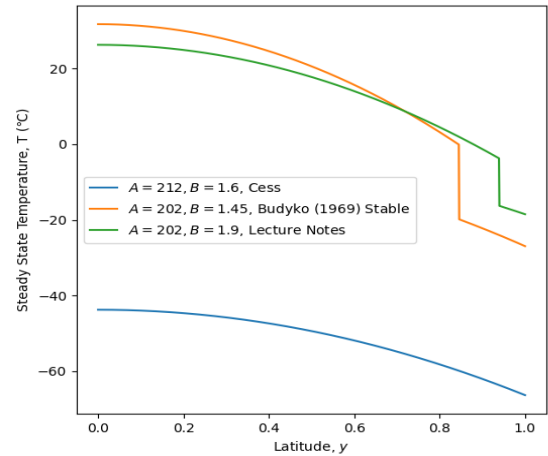


Figure 8: Temperature steady states for differing parameters  $A$  and  $B$

As expected, we see that the ice-covered steady state predicted by Cess'  $A$  and  $B$  values for the fixed solar constant value  $Q_0 = 342 \text{ W m}^{-2}$  has a much lower temperature range than the mixed-state climate as projected by the original model. In the case of Budyko's 1969 parameters, we see that the minimum temperatures are indeed lower than the original model's, as expected due to the

ice line being at a lower latitude. However, interestingly we see that the temperature at the equator is actually higher than the original model, possibly due to the value of  $B$  being lower, which changes the transport coefficient  $k = 1.6B$ , in turn reducing the diffusion of heat from the equator to the poles.

## Investigation 2

### (a) Asymmetric Steady States

In order to study undiscovered steady and non-steady states, we must consider the limitations of our model. Currently, we assume the Earth is symmetric about the equator and all factors are modelled independently of the longitudinal angle. In the following analysis we will see where these limitations are detrimental to our model.

We will start by analysing real world data against our model, we load in a dataset<sup>[4]</sup> and visualise the data. We are interested in how albedo actually changes globally, as currently our discontinuous step function is naive to the fact that landmass has a lower albedo than oceans.

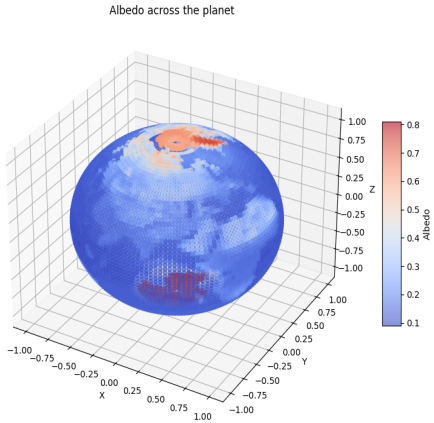


Figure 9: Measured values of albedo globally

We can clearly see large global landmasses and one of the most notable, the Saharan desert in Africa. Similarly, we are able to see Europe and it's associated higher albedo than the surrounding oceans. We compare our step function's behaviour over different latitudes when compared to the measured mean values.

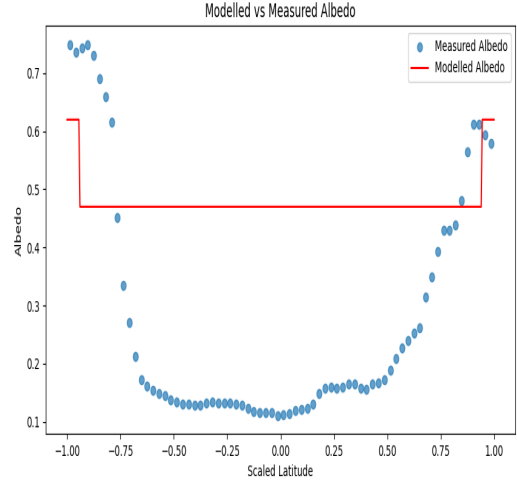


Figure 10: Measured values of albedo globally.

We can see a notable difference in the values, with the actual albedo around the equator being around 0.15 compared to a modelled 0.48. We are also able to distinguish a notable difference in albedo between the North Pole and Antarctica, which could be because Antarctica ( $y = -1$ ) is a landmass with ice on it, whereas the North Pole is a sea covered in ice.

We continue by fitting a model to our data using a GAM (generalised additive model)<sup>[5]</sup> and employing SciPy's quadrature method to find a solution to  $\bar{a}$ . We find  $\bar{a} \approx 0.5546$ .

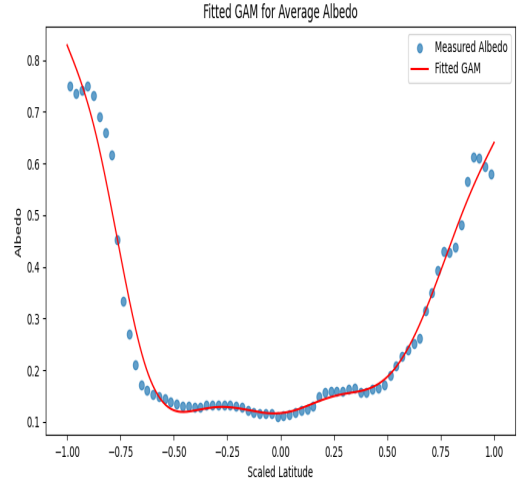


Figure 11: A fitted Generalised Additive Model for Albedo

We now consider the asymmetric steady states of the Earth's temperature. For this part of the analysis, we will assume a fixed ice line  $y_s = 0.813$  as given in this article<sup>[6]</sup>. We note that this value fits with our above estimations.

Recall the steady state value of temperature from lecture notes (16.6) given as the following:

$$T_{\infty}(y) = \frac{Q}{B+k} [s(y)(1-a(y)) + \frac{k}{B}(1-\bar{a})] - \frac{A}{B} \quad (1)$$

We now look to model temperature across both the Northern and Southern Hemispheres. There is however, extra steps to consider. Since we are now modelling the global temperature instead of just the equator to the North Pole, we must take care to properly evaluate our model with the appropriate parameters. As this study<sup>[7]</sup> suggests the outgoing radiation  $E_{out}$  should be split by Northern and Southern Hemisphere explicitly:

$$E_{out} = \begin{cases} 257 + 1.63T - (91 + 0.11T)A_c & \text{For } y \in [0, 1] \\ 262 + 1.64T - (81 + 0.09T)A_c & \text{For } y \in [-1, 0] \end{cases}$$

Here we introduce a new term  $A_c$ , which is the cloud cover fraction. It was found in<sup>[8]</sup> that the cloud cover fraction in the Northern Hemisphere was 63.5% and 68.5% in the Southern Equator. For the simplicity of our model, we assume a constant cloud cover independent of longitude. Using this information, we devise our temperature model 1 with revised coefficients  $A_{North} = 199.215$ ,  $B_{North} = 1.56015$ ,  $A_{South} = 206.515$ ,  $B_{South} = 1.57835$ . We model the temperature for the North and South hemisphere independently, then flip the South hemisphere temperature over to the region  $y \in [0, 1]$  in order to compare the Northern and Southern Hemisphere temperatures.

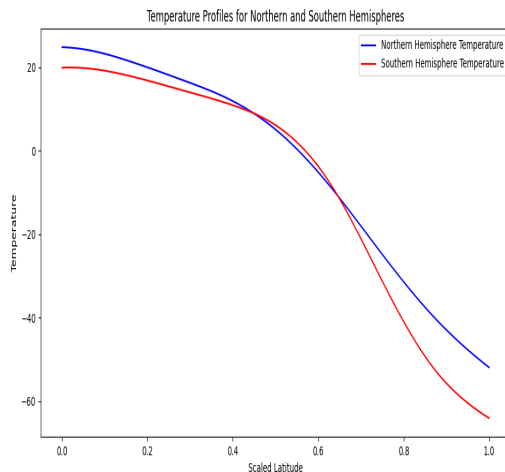


Figure 12: Modelled Temperatures

We analyse that at the poles, the Northern hemisphere is warmer. This can be explained by the lower albedo in the Arctic circle compared to Antarctica. Furthermore, our results agree with prevailing research<sup>[10]</sup> which indicates the Northern Hemisphere has a higher temperature than the south. The difference in temperatures between the two hemispheres implies the existence of asymmetric steady states.

We notice discontinuity at the equator ( $y = 0$ ), where the Northern Hemisphere is approximately  $4^{\circ}\text{C}$  warmer than the Southern Hemisphere. We can deduce this difference is a result of using different cloud cover fractions for each hemisphere. While our revised model does a better job at determining temperatures, it does not take into several key factors such as seasonal changes, altitude and longitudinal trade winds circulating warm weather fronts.

## (b) Continuous Albedo Function

We now employ a continuous analytical function for albedo, allowing us to quantify differences in our temperature model compared to using the step function approach suggested by Budyko. We use an adapted formula as originally proposed by Zaliapin and Ghil (2010)<sup>[11]</sup>, but with modified coefficients made popular by the University of Bath's very own Professor Chris Budd and Matt Griffith.<sup>[12]</sup>

$$\alpha(T) = 0.495 - 0.205 \tanh(\kappa(T - T_c))$$

By varying  $\kappa$  we analyse the following:

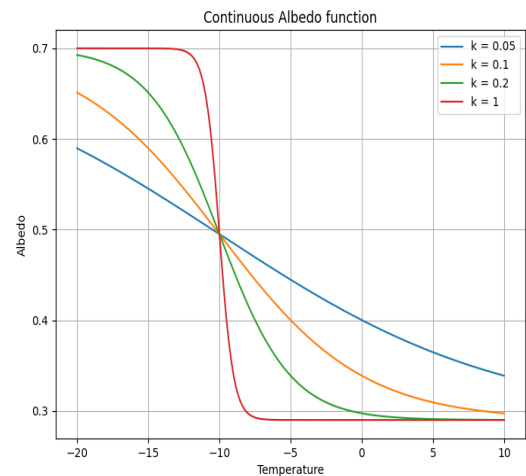


Figure 13: Albedo Function



This model can be implemented effectively because it is an albedo function explicitly dependent on temperature, and not implicitly through the location of the ice line  $y_s$ . We aim to analyse the difference in steady states given by this function and therefore consider the scenario where  $E_{in} - E_{out} = 0$  given by  $Q[1 - \alpha(T)] - \sigma\gamma T^4 = 0$ .

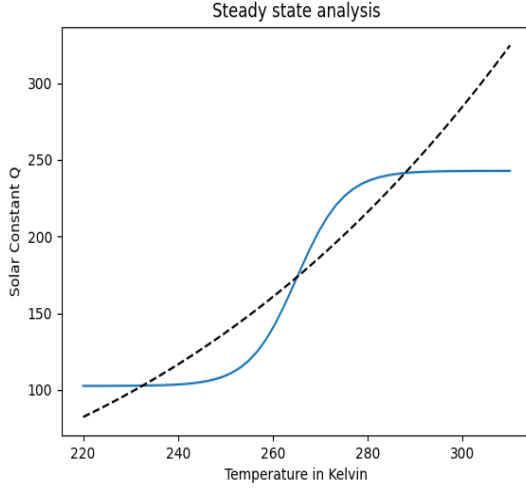


Figure 14: Steady States for a continuous albedo function

We see we have 3 steady states corresponding to different scenarios on Earth. The first is given by  $T_1 = 232.55K$ , which is a stable state with slow dynamics, this is often referred to as the Snowball Earth Scenario. Next, we have an unstable state given by  $T_2 = 265.15K$  as an 'intermediate' climate. Finally, we have the hot earth scenario which we are currently in. This is a stable steady state given by  $T_3 = 287.86K$ . Overall, we find very similar results with using a continuous albedo function compared to a discontinuous one.

## Investigation 3

### (a) Formulating real diffusion

We aim to now consider a real diffusion model given by the change  $E_{transport}(y, t) = \kappa \nabla^2 T$  where  $\nabla^2$  is the three dimensional Laplacian operator and  $\kappa$  is thermal diffusivity. We start by converting the problem into spherical polar coordinates using the following Laplacian formula<sup>[13]</sup>:

$$\nabla^2 T = \frac{1}{r^2} \frac{\partial}{\partial r} \left( r^2 \frac{\partial T}{\partial r} \right) + \frac{1}{r^2 \sin^2(\theta)} \frac{\partial^2 T}{\partial \phi^2} + \frac{1}{r^2 \sin(\theta)} \left( \frac{\partial}{\partial \theta} \left( \sin(\theta) \frac{\partial T}{\partial \theta} \right) \right)$$

where we define  $r$  = radius,  $\phi$  = Long. angle,  $\theta$  = Lat. angle from the North Pole.

Since we are measuring from the North Pole, we have  $y = \sin(\frac{\pi}{2} - \theta) = \cos(\theta)$ . We are measuring from the surface of the earth only, so  $r = 1$  and  $\frac{\partial T}{\partial r} = 0$ . Since in this model the heat distribution will be assumed homogeneous over the Longitudinal angle, implying  $\frac{\partial^2 T}{\partial \phi^2} = 0$ . Therefore,

$$\nabla^2 T = \frac{1}{\sin(\theta)} \left( \frac{\partial}{\partial \theta} \left( \sin(\theta) \frac{\partial T}{\partial \theta} \right) \right)$$

We apply the chain rule several times below to gain the required form

$$\begin{aligned} \nabla^2 T &= \frac{1}{\sin(\theta)} \left( \frac{\partial}{\partial \theta} \left( -\sin^2(\theta) \frac{\partial T}{\partial y} \right) \right) \\ &= \frac{1}{\sin(\theta)} \left( -\sin(\theta) \frac{\partial}{\partial y} \left( -\sin^2(\theta) \frac{\partial T}{\partial y} \right) \right) \\ &= \frac{\partial}{\partial y} \left( (1 - y^2) \frac{\partial T}{\partial y} \right) \end{aligned}$$

As required. We now formulate the steady-state solutions to the diffusive EBM to be:

$$\begin{aligned} 0 &= \kappa \frac{\partial}{\partial y} \left( (1 - y^2) \frac{\partial T}{\partial y} \right) \\ &\quad + Qs(y)(1 - a(y)) - (A + BT) \end{aligned}$$

for  $y \in [0, 1]$  as required by substituting this expression for  $\nabla^2 T$  into the steady state.

### (b) Investigating model changes

We now consider steady state solutions to the diffusive model using solvebvp, with an initial ice line of  $y_s = 0.94$  using an initial 'guess',  $T_{guess}$ , such that  $T_{guess}(0.94) = T_c = -10^\circ C$ .

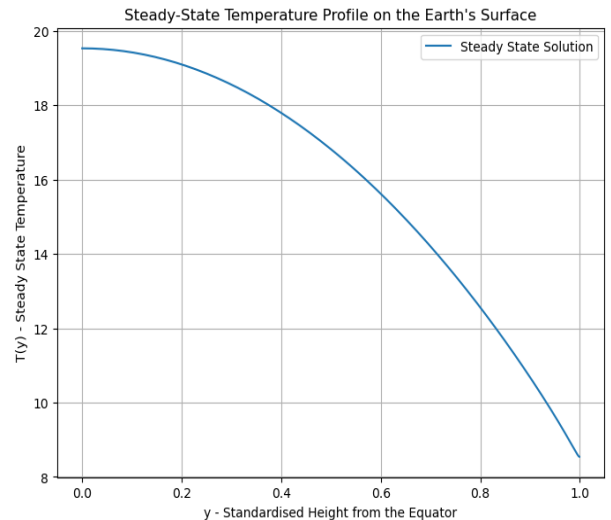


Figure 15: Steady-State Temperature Profile (initial  $y_s = 0.94$ )

While a diffusive model may be considered more realistic compared to the model prior, we observe solutions which are far worse at reproducing real data, suggesting a much smaller range of temperatures. This could be attributed to the nature of diffusion, which actively eliminates temperature gradients.

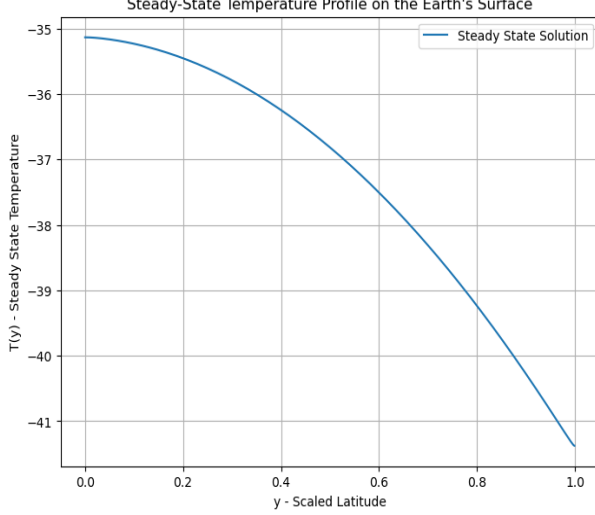


Figure 16: Steady-State Temperature Profile (initial  $y_s = 0$ )

The second steady-state temperature profile we obtain is a fully frozen over solution. The shapes of both plots are identical, but their scaling differs by a factor of roughly 1.76. The main challenge faced was obtaining partial-ice states using the full model. The dynamic albedo prompts solvebvp to overproduce mesh nodes in an attempt to correct inaccuracies, exceeding its capacity. To combat this, we noted that solutions typically failed to converge for initial  $y_s \approx 0.4$ , and modify the model making  $y_s$  a constant.

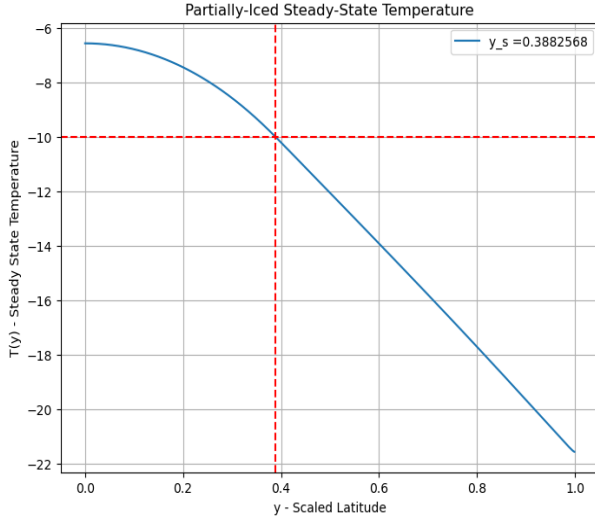


Figure 17: Partial Steady-State Temperature (with modified model,  $y_s = 0.388$ )

With this model, we found a partially iced state should exist for  $y_s = 0.388$ . It is also important to recognise that due to solvebvp using residuals to converge to stable solutions, it is not capable of accurately finding unstable solutions, which we know from Investigation 1 could exist.

## Varying The Solar Constant

We note first an important realisation for  $\bar{T}_\infty$ . Beginning with equation (6a), we integrate with respect to  $y$  over  $(0,1)$  which cancels out the energy transport expression due to the boundary conditions:

$$\int_0^1 \kappa \frac{\partial}{\partial y} \left( (1 - y^2) \frac{\partial T}{\partial y} \right) dy = \left[ (1 - y^2) \frac{\partial T}{\partial y} \right]_{y=0}^{y=1} = 0$$

Therefore we have

$$\begin{aligned} \int_0^1 Qs(y)(1 - a(y))dy &= \int_0^1 (A + BT)dy \\ \Rightarrow Q(1 - \bar{a}) &= A + B\bar{T}, \quad \bar{a} = \int_0^1 s(y)a(y)dy \\ \therefore \bar{T}_\infty &= \frac{Q(1 - \bar{a}) - A}{B} \end{aligned}$$

which is a similar relation as found in Investigation 1. Assuming  $y_s$  is unchanged,  $\bar{T}_\infty$  is linear in both  $Q$  and  $A$ , is inversely proportional to  $B$ , and is independent of  $\kappa$ . This is only observable for changes in the full-ice or full-water steady states.

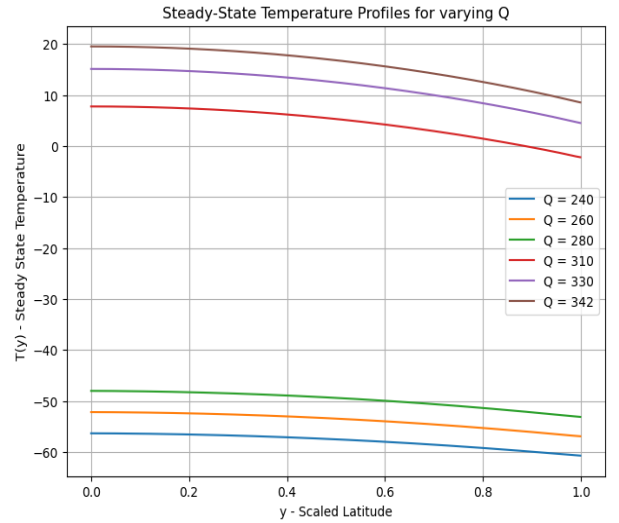


Figure 18: Steady-state Temperature Profiles with varying  $Q$  for initial  $y_s = 1$



Figure 18 illustrates the existence of the full-water steady state solution with respect to varying  $Q$ . We can infer that there must be a tipping point for  $Q \in (280, 310)$  where the full-water steady state disappears, similar to what was seen in investigation 1. For solutions in this region however, the model had difficulty converging because of a slow moving ice line causing the maximum nodes to be exceeded again. For that reason, we have used a simplification for the full water albedo, namely:  $a(y) = a_w, \forall y \in [0, 1]$ . This allows us to avoid the issues of the implicit model, and we find an approximate value of  $Q_{min} = 285.5 W m^{-2}$ , the minimum solar radiation  $Q$  for the full-water steady state to exist. Similarly, we can use  $a(y) = a_i, \forall y \in [0, 1]$  to analyse the full ice case. Using this, we find an approximate value of  $Q_{max} = 467.68 W m^{-2}$ , the maximum  $Q$  for the full-ice steady state to exist. The difference in these values is much more extreme than the values found in Investigation 1, but is expected given the range in temperature under the diffusive model is much smaller.

### Varying The Thermal Diffusivity

From our equation for  $\bar{T}_\infty$  we can also conclude, assuming  $y_s$  remains unchanged, that the mean steady state temperature is independent of  $\kappa$ .

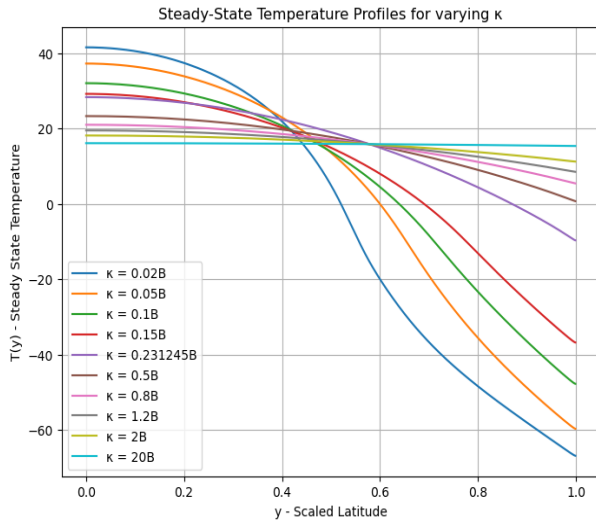


Figure 19: Steady-state Temperature Profiles with varying  $\kappa$  for initial  $y_s = 1$

For  $\kappa \gg 1$ , the diffusion becomes dominant with  $T(y) \approx 16.08^\circ C = \frac{Q(1-\bar{a}_w)-A}{B}$  as found before. As  $\kappa$  increases, it pivots around the point (0.57, 15.4) keeping the same mean temperature of  $16.08^\circ C$  until  $\kappa \approx 0.23B$  where the ice line begins to move away from the North Pole and

we see the mean temperature decreases. Note however that for  $\kappa < 0.23B$  the solutions did not converge accurately, but still describes an approximate trend. This same behavior is seen for the full ice steady state with a sharp rise in mean temperature for  $\kappa < 0.001B$ , where the ice line retreats from the equator. Comparing these plots to expected data values, it is also arguable that a more accurate value for  $\kappa$  is somewhere closer to  $0.5B$  or less.

## Conclusion

The report explored Earth's climate dynamics using an Energy Balance Model (EBM), focusing on temperature distribution and ice formation. Reducing the solar constant to  $325.8 W/m^2$  can trigger a fully glaciated state, while an increase to  $441 W/m^2$  leads to an ice-free state, indicating hysteresis in climate transitions. Varying the transport parameter,  $k$ , showed that a low transport parameter causes significant temperature variation across latitudes, with an ice line at  $y_s \approx 0.566$ , while a high transport parameter creates more uniform temperatures.

Changing the critical temperature ( $T_c$ ) affects ice coverage: above  $-6^\circ C$  leads to more ice, while below  $-12^\circ C$  suggests an ice-free state. Adjustments to parameters A and B, which govern outgoing energy, influence the ice line's position and overall climate stability. Budyko's later values suggest an ice line at  $y_s \approx 0.939$ , while other parameter sets, like Cess' 1976, point to different positions.

Using real-world albedo data, the report revealed significant asymmetries between the Northern and Southern Hemispheres due to cloud cover and albedo variations, impacting global temperatures. A continuous albedo function showed three steady states: snowball Earth at  $232.55 K$ , an unstable intermediate state at  $265.15 K$ , and a hot Earth state at  $287.86 K$ .

A diffusion-based EBM suggested high temperatures near the poles, indicating limitations with diffusion modeling, alongside difficulty in achieving well defined solutions. Nonetheless, key characteristics of the model are extractable akin to those in Investigation 1, such as relations involving mean temperature, expressing a linear relation to solar radiation and an independence of  $\kappa$  in regard to the full ice/water states. Varying the solar constant revealed critical tipping points also, with a minimum of  $285.5 W/m^2$  and a maximum of  $467.68 W/m^2$ .

# References

- [1] B Turner (Jul 2023) *Gulf Stream current could collapse in 2025, plunging Earth into climate chaos: 'We were actually bewildered'* Live science <https://www.livescience.com/planet-earth/climate-change/gulf-stream-current-could-collapse-in-2025-plunging-earth-into-climate-chaos-we-were-actually-bewildered>
- [2] IMDB (Apr 2024) *Ice Age* IMDB <https://www.imdb.com/title/tt0268380/>
- [3] A P Stevens (Nov 2023) *Will the Gulf Stream really shut down?* Woods Hole Oceanographic Institution <https://www.whoi.edu/oceanus/feature/will-the-gulf-stream-really-shut-down/>
- [4] Climate Data Information (2010-2020) *DiffAlbedo.csv* Climate data <http://www.climatedata.info/forcing/data-downloads/>
- [5] Wikipedia (Apr 2024) *Generalised additive model* Wikipedia [https://en.wikipedia.org/wiki/Generalized\\_additive\\_model](https://en.wikipedia.org/wiki/Generalized_additive_model)
- [6] A Shields, V S Meadows, C Bitz, R T.Pierrehumbert, M Joshi, T D Robinson (May 2013), *The Effect of Host Star Spectral Energy Distribution and Ice-Albedo Feedback on the Climate of Extrasolar Planets* ResearchGate [https://www.researchgate.net/publication/236965812\\_The\\_Effect\\_of\\_Host\\_Star\\_Spectral\\_Energy\\_Distribution\\_and\\_Ice-Albedo\\_Feedback\\_on\\_the\\_Climate\\_of\\_Extrasolar\\_Planetspg.15](https://www.researchgate.net/publication/236965812_The_Effect_of_Host_Star_Spectral_Energy_Distribution_and_Ice-Albedo_Feedback_on_the_Climate_of_Extrasolar_Planetspg.15)
- [7] R D. Cess (Oct 1976) *Climate Change: An Appraisal of Atmospheric Feedback Mechanisms Employing Zonal Climatology* American Meteorological Society [https://journals.ametsoc.org/view/journals/atsc/33/10/1520-0469\\_1976\\_033\\_1831\\_ccaaoa\\_2\\_0\\_co\\_2.xml](https://journals.ametsoc.org/view/journals/atsc/33/10/1520-0469_1976_033_1831_ccaaoa_2_0_co_2.xml)
- [8] Wikipedia (Apr 2024) *Cloud cover* Wikipedia [https://en.wikipedia.org/wiki/Cloud\\_cover](https://en.wikipedia.org/wiki/Cloud_cover)
- [9] K Mao, Z Yuan, Z Zuo, T Xu (Apr 2019) *Changes in Global Cloud Cover Based on Remote Sensing Data from 2003 to 2012* ResearchGate [https://www.researchgate.net/figure/Mean-cloud-cover-in-the-Northern-and-Southern-Hemispheres-from-2003-to-2012\\_fig1\\_331472729](https://www.researchgate.net/figure/Mean-cloud-cover-in-the-Northern-and-Southern-Hemispheres-from-2003-to-2012_fig1_331472729)
- [10] G Feulner, S Rahmstorf, A Levermann, S Volkwardt (2013) *Why is the Northern Hemisphere warmer than the Southern Hemisphere?* Astrophysics Data System <https://ui.adsabs.harvard.edu/abs/2013EGUGA..15.8172F/>
- [11] I Zaliapin, M Ghil (Mar 2010) *Another Look at Climate Sensitivity* arXiv <https://arxiv.org/pdf/1003.0253.pdf>
- [12] C Budd, M Griffith (Sept 2020) *Models of climate: Hot and Snowball Earths* University of Bath <https://people.bath.ac.uk/mascjb/PUSTalks/Autumn18a.pdf>
- [13] National Institute of Standards and Technology (Mar 2024) *Algebraic and analytical methods* National Institute of Standards and Technology <https://dlmf.nist.gov/1.5#E17>